Cooperative subnetworks of molecularly-similar interneurons in mouse neocortex

Mahesh M Karnani 1, Jesse Jackson 1, Inbal Ayzenshtat 1, Jason Tucciarone 2, Kasra Manoocheri 1, William G Snider 1, Rafael Yuste 1

1) Department of Biological Sciences, Columbia University, New York, NY 10027,
2) Cold Spring Harbor Laboratory, Cold Spring Harbor, New York 11724, MSTP/Neuroscience Graduate Program, Stony Brook University, Stony Brook, New York 11790

Corresponding author:
Mahesh Karnani, miikael.mmk@gmail.com

Supplemental Movies and Figures
Supplemental Experimental Procedures

Supplemental figure and movie legends.

Movie S1, related to Figure 1: Coactivity of VIPs in vivo.
Left panel, red channel image at 1040 nm excitation (VIP-cre::LSL-TOM). Right panel green channel movie at 940 nm excitation (syn-GCaMP6s), Kallmann filtered by two frames and sped up to 10 fps from the original 4 fps. Blue arrows denote VIPs without GCaMP and red arrows VIPs with GCaMP.

Movie S2, related to Figure 1: Coactivity of SOMs in vivo.
Left panel, red channel image at 1040 nm excitation (SOM-cre::LSL-TOM). Right panel green channel movie at 940 nm excitation (syn-GCaMP6s), Kallmann filtered by two frames and sped up to 10 fps from the original 4 fps. Blue arrows denote SOMs without GCaMP and red arrows SOMs with GCaMP.

Figure S1, related to Figure 1: Coactivity analysis from in vivo calcium imaging movies with high numbers of Interneurons. We used only stationary epochs for this analysis, since most data was available in this condition.
(A) Comparison of VIP coactive frames (red) to 'ISI-shuffled' surrogate data (black, plotted as mean ± 2*SD, see Methods for shuffling details) in an example movie lasting 4508 frames. Frames where a cell was active were defined by thresholding the delta-F/F traces with a mean+2*SD cutoff for each cell.
(B) Comparison of VIP coactive frames (red) to non-VIP coactive frames (blue, plotted as mean ± SD of 10 000 random subsamples from the non-VIPs) from same movie as in A.
(C) Summarized coactivity index (for each cell, the proportion of active frames where >2 other neurons in that category were active too) across 10 movies from 5 VIP-cre::LSL-TOM animals. Each imaged region had 7-12 GCAMP expressing and active VIPs.
(D) Comparison of SOM coactive frames (green) to 'ISI-shuffled' surrogate data (black, plotted as mean ± 2*SD, see Methods for shuffling details) in an example movie lasting 3483 frames.
(E) Comparison of SOM coactive frames (green) to non-SOM coactive frames (blue, plotted as mean ± SD of 10 000 random subsamples from the non-SOMs) from same movie as in D.
(F) Summarized coactivity index across 7 movies from 3 SOM-cre::LSL-TOM animals. Each imaged region had 7-10 GCAMP expressing and active SOMs.
In all panels, *, $P < 0.05$; †, $P < 0.0005$ with z-test in panels A, B, D, E and paired T-test in C and F.

Figure S2, related to Figure 2: Rabies tracing heat maps from each brain and laminar distribution of VIP-cre, SOM-cre and SOM-GFP(GIN) neurons.
(A) And (B) Average cell count heat maps from each brain used in Figure 2E and F.
(C) Example confocal micrographs and average cell count heat maps from S1 of VIP-cre::LSL-TOM, SOM- cre::LSL-TOM and SOM-GFP(GIN) (from a VIP-cre::LSL-TOM::SOM-GFP(GIN) animal) in coronal sections showing laminar distribution of these INs. (A-C) All scale bars are 200 μm.

Figure S3, related to Figure 3: Subthreshold membrane potential cross-correlograms for each neuron pair less than 150 μm apart, PV-PV and PV-SOM cross-correlograms, and PV pair L-EPSC assay.
(A) Cross-correlograms of individual cell pairs used in Figure 3D.
(B) Cross-correlograms of individual PV-PV (n = 5; 2 from S1, 3 from V1) and PV-SOM (n = 18; 6 from S1, 12 from V1) cell pairs.
(C) Data from B averaged, shaded area represents sem. Although we used the same 150 μm intersomatic distance cutoff on these recordings, the exact distances were PV-PV 88 ± 19 μm, PV-SOM 54 ± 8 μm ($P = 0.063$).
(D) 2-photon imaging protocol for separating SOM-GFP cells from CaMKII-C1V1-YFP cells used in Fig. 2B and Fig. 3E.
(E) 2-photon micrograph of two PVs recorded in PV-cre::LSL-TOM animal expressing CaMKII-C1V1- YFP. Asterisks on top of image represent 2-photon stimulation targets.
(F) Example trace from the PVs shown in E. L-EPSCs marked * are shared and those marked # are not shared between the cells.
(G) Comparison of shared and not shared L-EPSC counts from each experiment with VIP-SOM (n = 6, data re-plotted from Fig. 3G) and PV-PV pairs (n = 5). Shared and not shared counts from the same experiment are connected by a line and mean ± sem are shown next to the lines as black symbols with error bars. *, $P < 0.05$; †, $P = 0.00002$; N.S., $P = 0.90$ by z-test against zero.

Figure S4, related to Figure 4: Interneuron connectivity in S1 and V1.
(A) Connection probabilities in S1.
(B) Connection probabilities in V1.
(C) Connection probabilities in S1 and V1 combined.

Figure S5, related to Figures 4 and 5: Table chart of electrophysiological parameters of each cell type subcategorized by their connectivity or cooperative properties (VIPs only, * refers to Figure 5G,H during 3 cell firing and relevant text in Results, ** refers to Figure 5I left panel and relevant text in results). The arrow symbol -> denotes synaptic connection in the direction of the arrow while the symbol –x denotes lack of synaptic connection toward the x. V_M = resting membrane potential, R_M = input resistance, C_M = whole cell capacitance, V_{thresh} = action potential threshold, AP amp = action potential amplitude, AHP amp = after-hyperpolarization amplitude. There were no significant differences in any parameter within a cell type (VIP, n = 3-12; SOM, n = 6-12; PC, n = 6-8; or PV, n = 6-12) as tested by a T-test with P>0.05.

Figure S6, related to Figure 5: VIPs are more sensitive to ambient ACh than PVs and SOMs.
(A) Effect of bath applied 10 μM ACh on two VIPs and two SOMs recorded simultaneously in VIP-cre::LSL-TOM::SOM-GFP(GIN) slice.
(B) Effect of ACh on a PV and a PC recorded in different slices.
(C) Summary data from recordings like A and B, n = 4-8 cells for each datapoint. *, P < 0.05; N.S., P>0.05 by paired T-test. All data from V1.

FIG S1

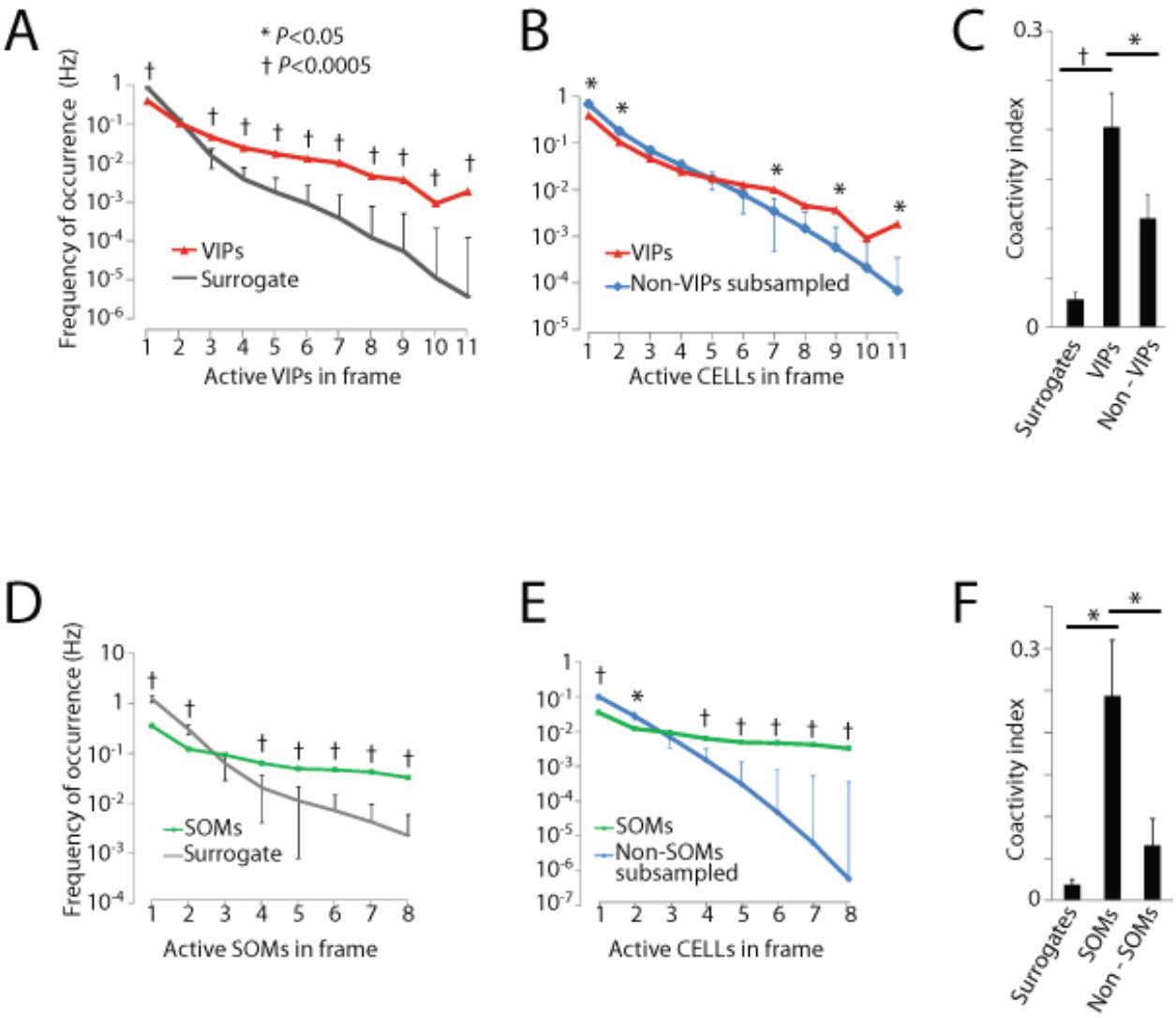
A
* P<0.05
† P<0.0005
Frequency of occurrence (Hz)
VIPs
Surrogate
Active VIPs in frame
B
VIPs
Non-VIPs subsampled
Active CELLs in frame
C
Coactivity index
Surrogates
VIPs
Non - VIPs
D
Frequency of occurrence (Hz)
SOMs
Surrogate
Active SOMs in frame
E
SOMs
Non-SOMs subsampled
Active CELLs in frame
F
Coactivity index
Surrogates
SOMs
Non - SOMs

FIG S2

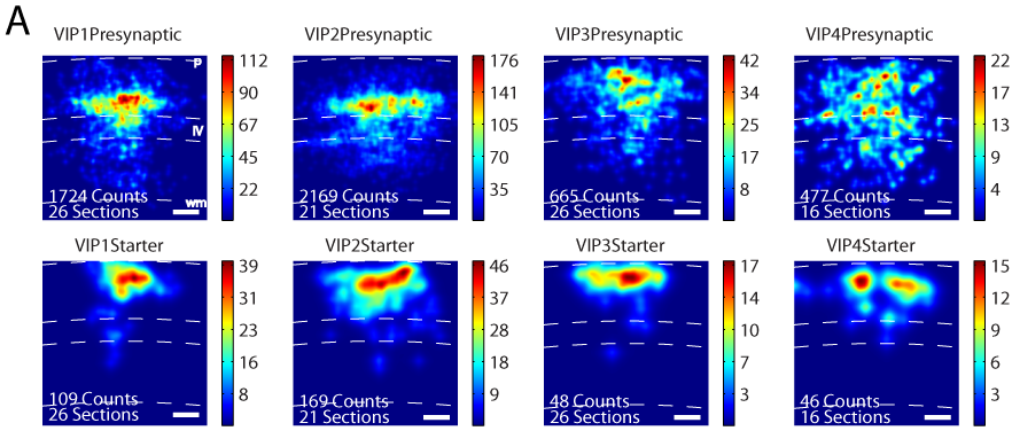
A
VIP1Presynaptic
1724 Counts
26 Sections
VIP2Presynaptic
2169 Counts
21 Sections
VIP3Presynaptic
665 Counts
26 Sections
VIP4Presynaptic
477 Counts
16 Sections
VIP1Starter
109 Counts
26 Sections
VIP2Starter
169 Counts
21 Sections
VIP3Starter
48 Counts
26 Sections
VIP4Starter
46 Counts
16 Sections

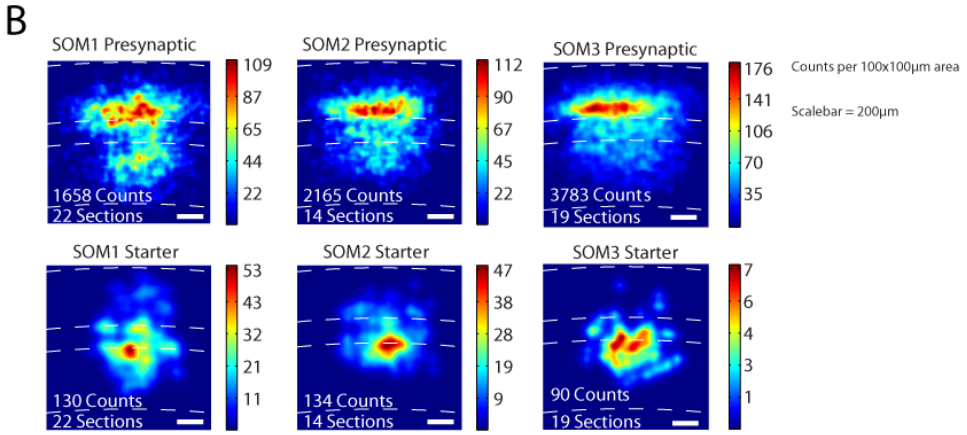
B
SOM1 Presynaptic
1658 Counts
22 Sections
SOM2 Presynaptic
2165 Counts
14 Sections
SOM3 Presynaptic
3783 Counts
19 Sections
Counts per 100x100µm area
Scalebar = 200µm
SOM1 Starter
130 Counts
22 Sections
SOM2 Starter
134 Counts
14 Sections
SOM3 Starter
90 Counts
19 Sections

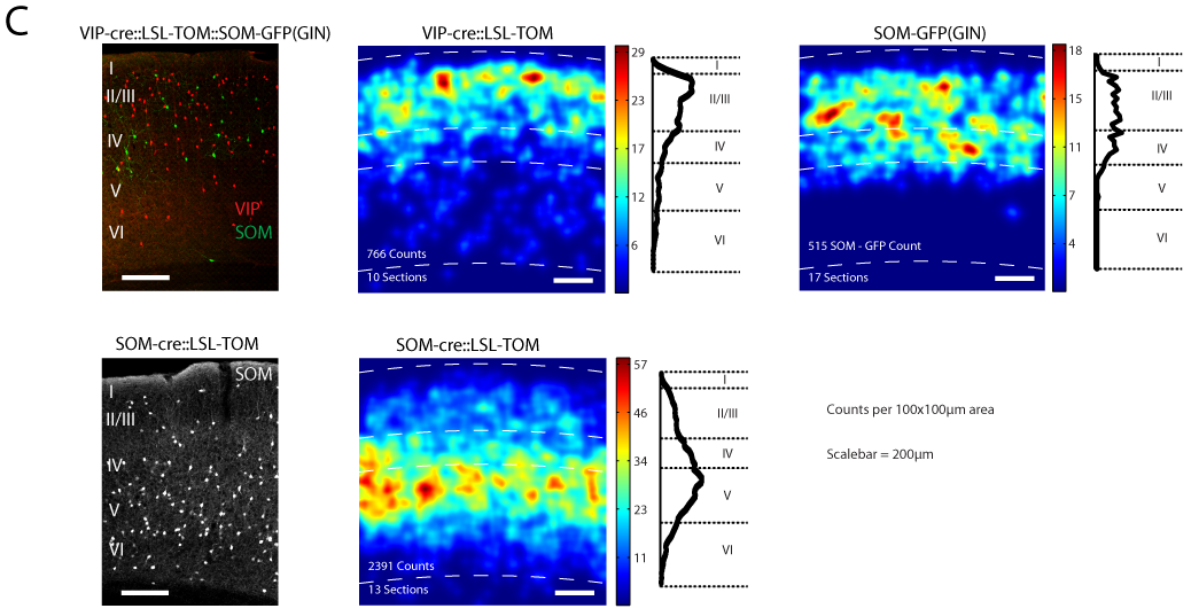
C
VIP-cre::LSL-TOM::SOM-GFP(GIN)
VIP
SOM
VIP-cre::LSL-TOM
766 Counts
10 Sections
SOM-GFP(GIN)
515 SOM - GFP Count
17 Sections
SOM-cre::LSL-TOM
SOM
SOM-cre::LSL-TOM
2391 Counts
13 Sections
Counts per 100x100µm area
Scalebar = 200µm

FIG S3

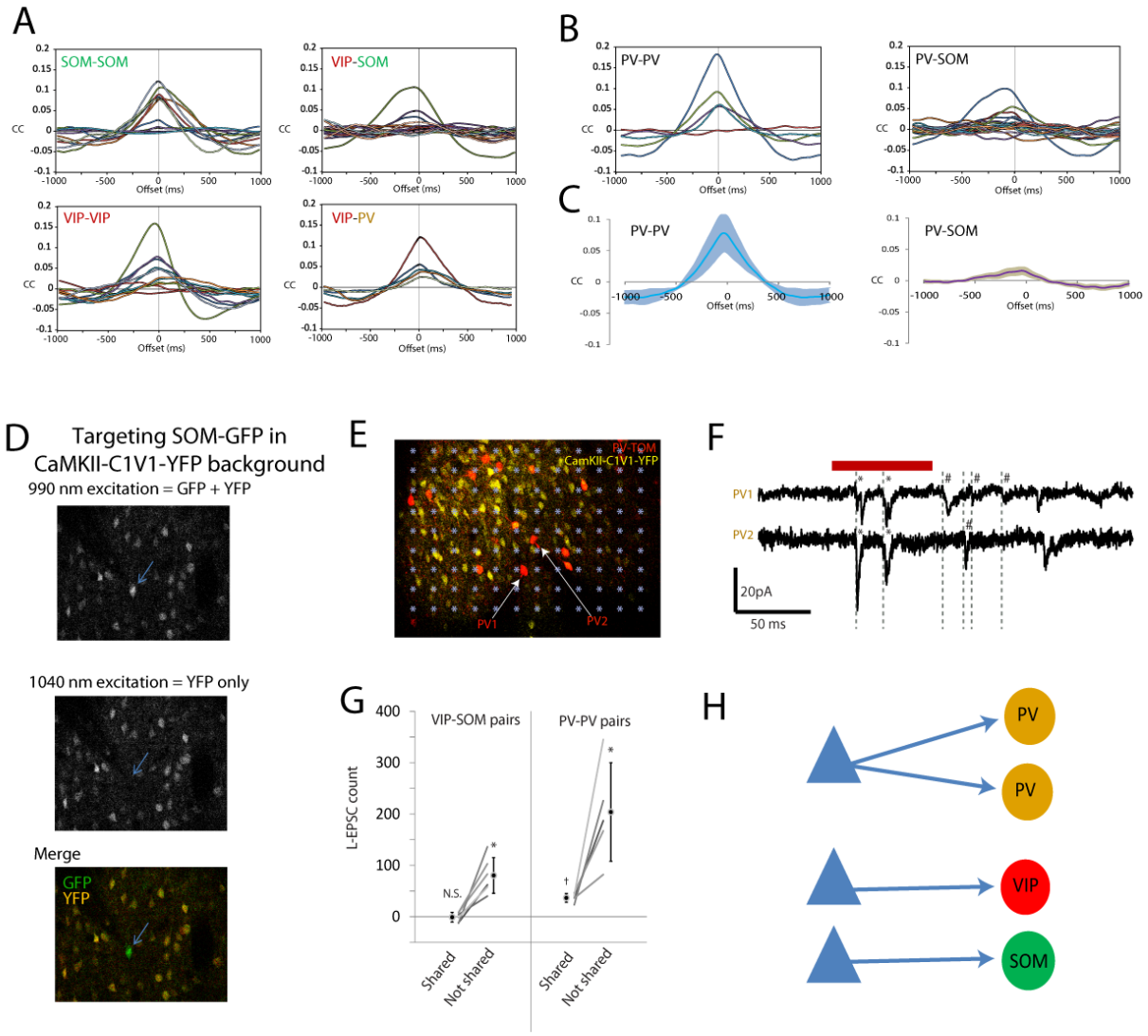
A
SOM-SOM
VIP-SOM
VIP-VIP
VIP-PV
CC
Offset (ms)
B
PV-PV
PV-SOM
C
PV-PV
PV-SOM
D
Targeting SOM-GFP in
CaMKII-C1V1-YFP background
990 nm excitation = GFP + YFP
1040 nm excitation = YFP only
Merge
GFP
YFP
E
PV-TOM
CamKII-C1V1-YFP
PV1
PV2
F
PV1
PV2
20pA
50 ms
G
VIP-SOM pairs
PV-PV pairs
L-EPSC count
N.S.
Shared
Not shared
H
PV
PV
VIP
SOM

FIG S4

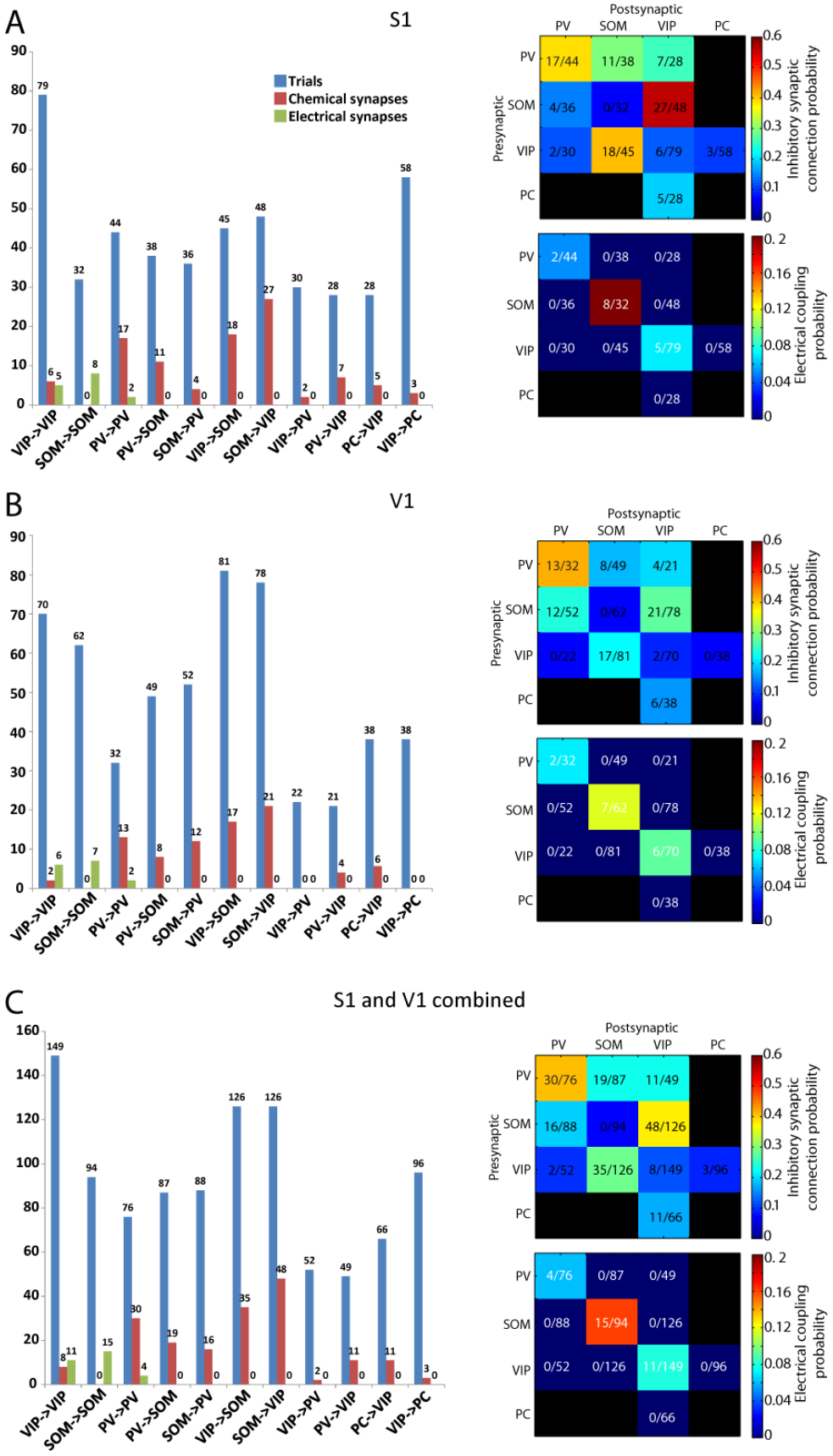
A
S1
Trials
Chemical synapses
Electrical synapses
VIP->VIP
SOM->SOM
PV->PV
PV->SOM
SOM->PV
VIP->SOM
SOM->VIP
VIP->PV
PV->VIP
PC->VIP
VIP->PC
Postsynaptic
PV
SOM
VIP
PC
Presynaptic
Inhibitory synaptic connection probability
Electrical coupling probability
B
V1
C
S1 and V1 combined

FIG S5

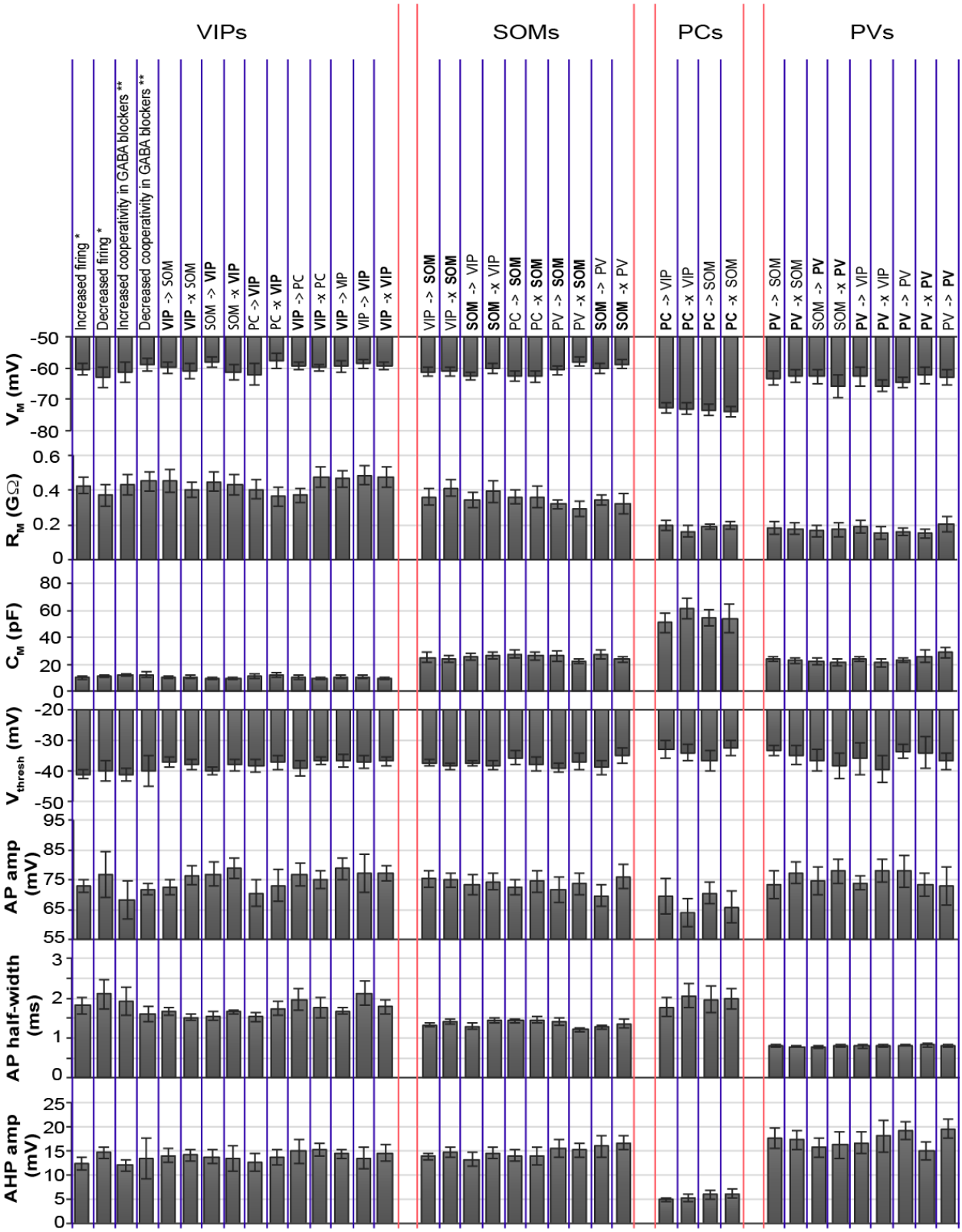
VIPs
SOMs
PCs
PVs
Increased firing *
Decreased firing *
Increased cooperativity in GABA blockers **
Decreased cooperativity in GABA blockers **
VIP -> SOM
VIP -x SOM
SOM -> VIP
SOM -x VIP
PC -> VIP
PC -x VIP
VIP -> PC
VIP -x PC
VIP -> VIP
VIP -x VIP
VIP -> SOM
VIP -x SOM
SOM -> VIP
SOM -x VIP
PC -> SOM
PC -x SOM
PV -> SOM
PV -x SOM
SOM -> PV
SOM -x PV
PC -> VIP
PC -x VIP
PC -> SOM
PC -x SOM
PV -> SOM
PV -x SOM
SOM -> PV
SOM -x PV
PV -> VIP
PV -x VIP
PV -> PV
PV -x PV
PV -> PV
V_M (mV)
R_M (GΩ)
C_M (pF)
V_{thresh} (mV)
AP amp (mV)
AP half-width (ms)
AHP amp (mV)

FIG S6

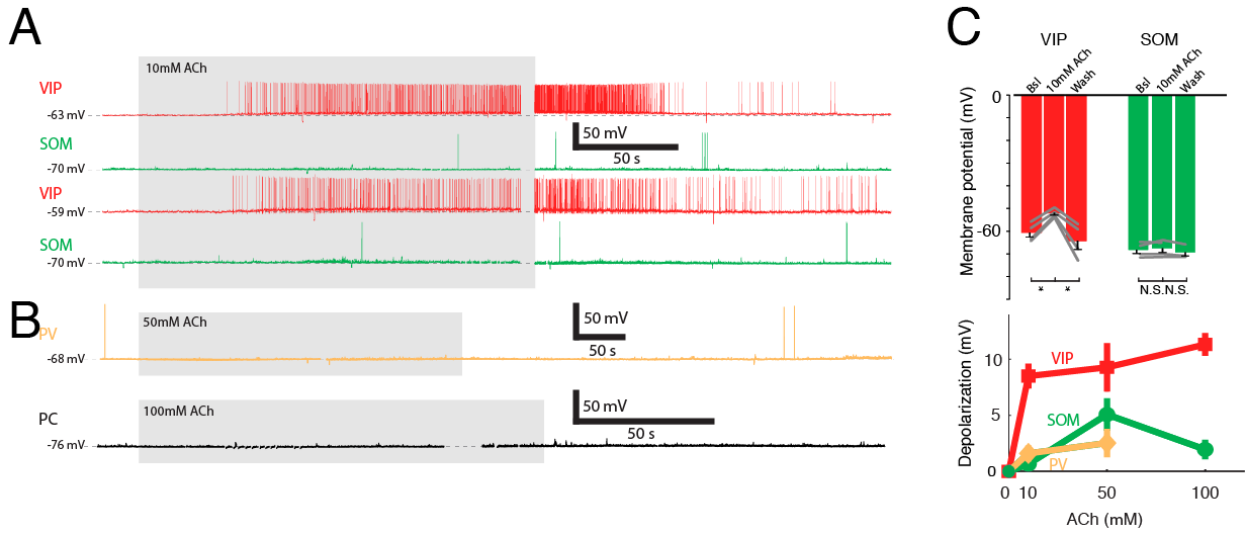
A
10mM ACh
VIP
-63 mV
SOM
-70 mV
VIP
-59 mV
SOM
-70 mV
50 mV
50 s
B
PV
-68 mV
50mM ACh
50 mV
50 s
PC
-76 mV
100mM ACh
50 mV
50 s
C
VIP
SOM
Bsl
10mM ACh
Wash
Membrane potential (mV)
0
-60
N.S.N.S.
Depolarization (mV)
10
5
0
VIP
SOM
PV
0 10 50 100
ACh (mM)

Supplemental Experimental Procedures

Animals

Animals of both sexes were used and were housed in a controlled environment on a 12h light-dark cycle with food and water ad libitum. VIP-cre (stock #010908, RRID:IMSR_JAX:010908), PV-cre (stock #017320, RRID:IMSR_JAX:017320), SOM-cre (stock #013044, RRID:IMSR_JAX:013044), SOM-GFP(GIN) (stock #003718, RRID:IMSR_JAX:003718), PV-GFP(G42) (stock #007677, RRID:IMSR_JAX:007677), LNL-tTA (stock # 008600, RRID:IMSR_JAX:008600) and LSL-tdTomato (LSL-TOM, Ai14, stock #007908, RRID:IMSR_JAX:007908) mice were obtained from the Jackson Laboratory and cross-bred to yield VIP-cre::LSL-TOM, SOM-cre::LSL-TOM and PV-cre::LSL-TOM. These were further crossed with the GFP lines to yield VIP-cre::LSL-TOM::SOM-GFP(GIN), VIP-cre::LSL-TOM::PV-GFP(G42) and PV-cre::LSL-TOM::SOM-GFP(GIN).

Surgery: Virus injections for calcium imaging and acute slice experiments

Three to four weeks prior to the experiments VIP-cre::LSL-TOM and SOM-cre::LSL-TOM mice were injected stereotactically with AAV1-syn-GCaMP6s (UNC vector core) for in vivo experiments (Figure 1), and VIP-cre::LSL-TOM::SOM-GFP(GIN) or PV-cre::LSL-TOM mice were injected with AAV5-CaMKIIα-C1V1(E162T)-p2A-EYFP (UNC vector core) for slice experiments (Figure 2B, 3E-H, S3D-G). Mice were anesthetized with isoflurane, the scalp was infiltrated with lidocaine, and a 0.1 × 0.1 mm craniotomy was drilled 2.5 mm lateral from lambda in the left hemisphere. An injection needle was slowly lowered to 150-200 μm below the pial surface and 500-1000 nl of virus was injected at a rate of 80 nl/min. After removal of the injection needle, the scalp was sutured and animals received 5mg/kg carprofen injections for three days as post-operative pain medication.

Surgery: *In vivo* experiments

Two weeks after viral delivery mice were anaesthetized with isoflurane, the scalp infiltrated with lidocaine and a custom-made titanium head plate was attached to the skull using dental cement. A 2 × 2 mm area of skull above the left V1 was partially thinned with a drill and covered with a silicone polymer. The mice received single doses of anti-inflammatory drugs (0.6mg/kg dexamethasone and 5mg/kg enrofloxacin) as well as 5mg/kg carprofen injections for three days as post-operative pain medication and over the following week were briefly trained for head-fixed awake experiments in 2-3 sessions of increasing length on the experimental running-wheel apparatus.

In vivo experiments

On the day of the experiment P60-120 mice were anaesthetized with isoflurane and the skull was thinned to < 100 μm. The animal recovered from this brief (< 0.5 h) surgery for 1 h and was then imaged in a dark room for 2-3 h head-fixed on a running disk allowing the animal to move or remain stationary ad libitum. Throughout imaging sessions, we recorded the movement of the running disk via a custom-built infra-red optical mouse apparatus to distinguish between movement and stationary epochs.

Two-Photon Ca^{+2} Imaging

Changes in GCaMP6s fluorescence were imaged with a Two-photon Moveable Objective Microscope (Sutter) and a mode-locked Ti:sapphire laser (Chameleon Vision II, Coherent) at 950 nm through a 25 x (1.05 NA, Olympus) water immersion objective at 4.07 fps with 512 x 512 pixels resolution using Mscan software (Sutter). Images were obtained with a 535/50 and 610/75 nm band-pass emission filters for the green and red channels, respectively. Each field-of-view (FOV) contained 4-19 Ca2+ indicator filled VIPs or SOMs.

Calcium imaging analysis

Motion artifacts and drifts in the imaging plane were corrected using TurboReg plug-in in ImageJ. Initial image processing was carried out using custom-written software in MATLAB. Cell outlines were drawn manually. Mean intensity within each region of interest (ROI) was used for *raw* $\Delta F/F$ by comparing to the previous 10 seconds. The ΔF/F used for analyses in Figure 1 was obtained by subtracting from each cell's *raw* $\Delta F/F$ its neuropil signal (defined as the 0.7**raw* $\Delta F/F$ of the extracellular space between the 300-500th closest pixels that did not include another ROI). Binarized data were obtained by using a mean+2*SD cutoff for each cell and defining a cell as active in a frame if its ΔF/F was above this threshold. Locomotion epochs were defined as the time when the mouse moved >1 cm/s (20 optical mouse pulses/ frame) along with the 5 seconds before and after these bouts, since locomotion and its onset and offset are known to modulate V1 neurons (Fu et al., 2014, Polack et al., 2013, Reimer et al., 2014, Vinck et al., 2015). Pairwise correlations were computed using Pearson's correlation to get data in correlation matrices in Figure 1 C,D,G,H. Pairwise correlations were averaged within each category to get mean data in Figure 1 C,D,G,H. Surrogate data in Figure S1 were generated for each movie from the binarized and locomotion-deleted VIP or SOM traces by

two shuffling methods that yielded essentially identical results: In inter-spike-interval shuffling (example data shown in Figure S1A,D) the intervals between chunks of continuously active frames were shuffled randomly within each cell's trace. The order of shuffling was different for each cell. In time-shift shuffling (data not shown) each cell's trace was shifted in time by a randomly chosen integer number of frames between one and the length of the movie. The time-shift was different for each cell. To generate a distribution of surrogate data, the shuffling was performed 1000 times starting each time from the experimental data. The 'co-activity index' in Figure S1 C,F was computed for each cell by dividing the number of frames in which it was active with more than 2 other cells of its class (VIP, non-VIP, SOM or non-SOM), by the total number of active frames for the neuron. These values were averaged across each cell in a movie and then averaged across movies resulting in the data shown in Figure S1 C,F.

Preparation of acute slices

Coronal brain slices from P21-180 animals were prepared after instant cervical dislocation and decapitation. The brain was rapidly dissected and cooled in continuously gassed (95% O_2 and 5% CO_2), icy cutting solution containing (in mM): 90 N-methyl-D-glucamine, 20 HEPES, 110 HCl, 3 KCl, 10 $MgCl_2$, 0.5 $CaCl_2$, 1.1 NaH_2PO_4, 25 $NaHCO_3$, 3 pyruvic acid, 10 ascorbic acid and 25 D-glucose. 300 µm thick coronal brain slices were cut on a vibratome (Microm) and allowed to recover for 5-15 min at 37 °C in cutting solution, followed by 45-55 min at 37 °C in standard artificial cerebrospinal fluid (ACSF) containing (in mM): 126 NaCl, 3 KCl, 2 $MgSO_4$, 2 $CaCl_2$, 1.1 NaH_2PO_4, 26 $NaHCO_3$, 0.1 pyruvic acid, 0.5 L-glutamine, 0.4 ascorbic acid and 25 D-glucose, always continuously gassed with 95% O_2 and 5% CO_2.

Slice electrophysiology

Patch clamp recordings were performed in a submerged chamber with 5-10 ml/min superfusion of either standard ACSF or a modified high K-ACSF (Figure 3A-D, 5) containing (in mM): 126 NaCl, 4 KCl, 1 $MgSO_2$, 3 $CaCl_2$, 1.1 NaH_2PO_4, 26 $NaHCO_3$, 0.1 pyruvic acid, 0.5 L-glutamine, 0.4 ascorbic acid 0.001 N-methyl-D-aspartate and 25 D-glucose, continuously gassed with 95% O_2 and 5% CO_2. 4-8 MOhm patch pipettes were filled either with a K-gluconate (for current clamp) or Cs-methylsulphonate (for voltage clamp) based intracellular solution. The K-gluconate intracellular contained (in mM): 130 K-gluconate, 5 NaCl, 2 $MgSO_2$, 10 HEPES, 0.1 EGTA, 4 Mg-ATP, 0.4 Na-GTP, 7 phosphocreatine, 2 pyruvic acid, 0.1 Alexa594, 0.2% biocytin, and ~10 mM KOH (to set pH to 7.3). The Cs-methylsulphonate intracellular solution was identical except for the substitution of 130 mM K-gluconate with 130 mM Cs-methylsulphonate. Gabazine (SR-95531) hydrobromide, CGP 35348 and mecamylamine hydrochloride were bought from Tocris and dissolved in ACSF. Whole cell recordings were not analysed if the access resistance was above 25 MOhm. Cells were identified with an upright microscope with 40X water immersion objective (0.8 NA, Olympus) and fluorescence optics. Voltage and current recordings were sampled at 10 kHz and low-pass filtered at 4 kHz with MultiClamp 700B amplifiers and acquired in LabView with custom software. Most recordings were performed at 24 °C for increased stability. Datasets in Figure 5 and 2A,B contain recordings at 35-37 °C (which were not different from recordings at 24 °C), performed to ensure that temperature effects do not confound our main conclusions. In Figure 5, when necessary, cells were injected sustained current of < 50 pA to maintain average firing rates between 1 – 10 spikes/3 s (average during 3 s before induced firing was 4.6 ± 0.3 spikes/3 s). In the GABAergic blockade experiments for Figure 5, ~70% of recordings developed epileptiform activity seen as global 0.5-1 s bursts occurring at a mean frequency of 0.1-0.001 Hz. Trials containing these bursts in the analysis windows were removed from analysis. In Figure 3C,D and S3A-C the recorded cells were injected up to 100 pA current to keep their firing to a minimum. The amount of injected current was not changed during recordings in Figs 3A-D, 5 or S3A-C.

Photo-stimulation

CaMKIIα-C1V1 was stimulated with green light from a mercury lamp through neutral density filters and a TRITC-filter cube. Timing was controlled with a shutter (Uniblitz). 2-photon mapping in Figures 3E-H and S3E-G was performed on a custom modified Olympus microscope coupled to a Chameleon Vision II laser, pockels cell, shutter and galvanometer mirrors. The experiment was controlled by custom software written in Matlab and LabView. 108 targets were arrayed in a 175 x 250 µm grid pattern with the recorded cells in the center and the targets were illuminated with the laser in a randomized order with 2 s intervals between targets. Each stimulation target contained 22 equally spaced micro-targets within a circle of 6 µm radius (comprising the target, * in Figure 3E and S3E), and the laser was targeted to each micro-target in a spiral sequence lasting 65 ms in total. For stimulation the laser was tuned to 1040 nm and power on sample was 20-40 mW.

Electrophysiology analysis
Most patch clamp data were analyzed with custom routines in Matlab. In Figure 5C and G, we categorized the response of a recorded cell by two separate comparisons: the firing rate during the induced firing train compared to 1) before and 2) after it in the firing rate histogram averaged across 9-21 trials. Recorded cells were categorized as 'increased firing' if there were more APs during the train compared to the three seconds both before and after the train, 'decreased firing' if there were less APs during the train compared to both before and after the train, and 'no change' if the difference between firing during the train compared to before had opposite sign of firing during the train compared to after. EPSCs in Figures 3E-H and S3E-G were detected semi-manually in Minianalysis (Synaptosoft). Cross-correlation data in Figure 3C,D and S3A-C were obtained from continuous current clamp traces lasting 285-1860 s by first deleting from all simultaneously recorded traces, epochs with action potentials along with the 10 ms before and 100 ms after the times when any trace crossed 0 mV. This procedure eliminated < 5 s from each trace. After this the traces were high-pass filtered above 0.0005 Hz to remove slow components due to electrode potential drift that can bias the analysis, and then cross-correlograms were generated.

Immunohistochemistry
Mice were overdosed with ketamine/xylazine (100mg/kg and 10mg/kg respectively) and transcardially perfused with 4% PFA. Brains were post-fixed for 24 h. Coronal brain slices were sectioned at 75 microns using a vibratome. Sections were blocked in PBS with 0.5% Triton X-100 and 10% bovine serum albumin (blocking solution) for 1 h, incubated with chicken anti-GFP (1:1000; Aves) over-night, washed, incubated with AlexaFluor488 goat anti-chicken secondary antibody (1:500; Molecular probes) for 4 h. Rabbit polyclonal anti-RFP antibody (1:1,000, Rockland) was used with AlexaFluor594 goat anti-rabbit secondary antibody (1:500, Molecular Probes) to enhance and preserve the rabies mCherry signal. Antibodies were applied in blocking solution. Confocal micrographs were merged in imageJ and quantified manually. For VIP immunohistochemistry, the same staining protocol was used with the exception of perfusion and post-fixation with 2% PFA and antibodies were rabbit anti-VIP (1:300, Immunostar) and biotin goat anti-rabbit (1:300, Molecular probes). The signal was developed with standard ABC and DAB kits (Vector Labs).

Rabies tracing analysis
Locations of presynaptic and starter cells were annotated in CellCounter plugin in ImageJ, followed by processing in Matlab with custom routines. The location data from each coronal section near the injection site (rostro-caudal span ~2 mm) from a brain were aligned by the pial contour and summed to get the heatmaps in Figure S2. These were then averaged across animals for the data in Figure 2F.